EXTRACTION OF PLASTIC PROPERTIES FROM THE INSTRUMENTD INDENTATION DATA: CURRENT STATUS

U. RAMAMURTY[1] and N. CHOLLACOOP[2]

[1]Department of Metallurgy, Indian Institute of Science, Bangalore – 560 012, India.

[2]Department of Materials Sci. and Engineering, Massachusetts Institute of Technology, Cambridge, MA 02139, USA.

ABSTRACT

An important aspect of the elastic-plastic analyses of sharp indentation will be the estimation of the representative strain, ε_r, underneath the indenter, which varies as a function of the tip geometry. Wide range of values for ε_r has been proposed in the literature. Recently, algorithms, developed on the basis of extensive large-strain finite element analyses, that enable the extraction of elastic and plastic properties from the instrumented pyramidal indentation data have been developed. Experiments that are conducted to critically assess the predictive capability of the reverse algorithms and in turn the ε_r values are presented.

1 INTRODUCTION

Depth-sensing indentation has become a popular technique in the recent past for mechanical property evaluation of thin films, coatings, and biological materials. In a typical instrumented indentation test, the *P-h* data are continuously recorded for a complete cycle of loading and unloading and are analyzed. During indentation, the material underneath the indenter experiences a pile-up or sink-in against the faces of the indenter, depending on many material parameters. Hence, it is difficult to measure the true contact area and considerable research has been conducted to overcome this. Standardized methodologies that circumvent this problem are now available which make it possible to evaluate properties such as the elastic modulus, *E*, and hardness, *H*, of a given material routinely. Similar methods for the extraction of plastic properties such as yield stress, σ_y, and the work hardening exponent, *n*, of metallic materials from the *P-h* curves, however, have been proposed. Elastic-plastic analyses of sharp indentation have been reported in the context of small strain finite element simulations. Results of such analyses have been used to develop forward and reverse analyses algorithms. While the forward algorithm predicts the *P–h* curve with the materials' elasto-plastic properties as input parameters, the reverse algorithm predicts materials' elasto-plastic properties from the experimentally measured *P–h* curves. Experimental work on a variety of metals shows that the extracted values of σ_y and *n* deviate significantly from those measured in uniaxial compression tests, indicating that further refinements to the modeling are necessary. Recently, Dao et al. [1] have conducted a comprehensive computational study and identified a set of analytical functions that take into account the pile-up/sink-in effects within the framework of large-strain finite element analysis (LFEA) of Berkovich indentation on power-law hardening elastic-plastic solids. Further, they identified a representative plastic strain, ε_r, as a strain level that allows for the description of the indentation loading response, independent of the work hardening exponent. On this basis, they proposed a methodology to assess properties of materials within the context of single [1] and dual [2] indentations. A critical experimental assessment of these methods is conducted in this work by indentation experiments on two metallic materials with distinct mechanical response.

2 MATERIALS AND EXPERIMENTS

Two materials were used for the experimental investigation: a highly cold-worked pure copper and an aluminum 6061-T651 alloy that was fully annealed to obtain the highest hardening. Uniaxial tensile tests were conducted on a screw-driven universal testing machine at a cross-head speed of 1.27 mm/min. The copper specimens was strained to ~1.6, 4, 7.3 and 10% engineering strain before unloading (labeled Cu1, Cu2, Cu3 and Cu4, respectively) whereas the aluminum specimens was strained to ~ 0.8, 3, 5 and 7% engineering strain (labeled Al1, Al2, Al3 and Al4, respectively). Specimens for the indentation were machined from the gage section of each strained specimen and from the grips of Cu1 and Al1 (labeled Cu1gs and Al1gs, respectively) which were used to assess the as-received material's indentation response. All the specimens were polished to 1 μm finish with diamond paste. The Cu1gs and Al1gs section of specimens were polished deeper than other specimens to completely remove the surface layer that is strained due to gripping. The polished samples were indented using an instrumented microindenter (MicroMaterials, Wrexham, UK) with a Berkovich and a 60° cone equivalent three-sided pyramid diamond tips at a loading rate of 0.1 N/s. It is important to note here that the depth of penetration recorded by the instrumented indenter also includes the displacement associated with the load train as a result of the machine compliance. Displacement associated with this single-valued machine compliance (estimated using the indentation of fused silica with known Young's modulus) is subtracted from the experimental data and the modified *P-h* curves were analyzed using the reverse algorithm.

3 RESULTS AND DISCUSSION

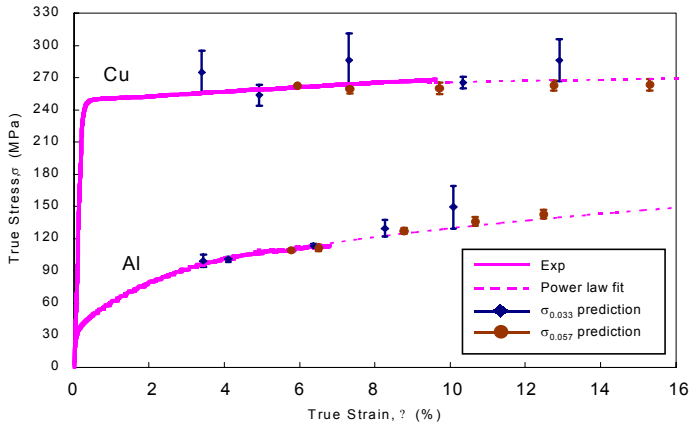

Figure 1: True stress-true strain curves generated through the uniaxial tensile tests. The values of the representative stresses, extracted using the reverse algorithms and offset by the prior plastic strain, are also plotted for comparison.

Table 1. Averaged mechanical properties determined from tensile tests with comparison with the extracted value from indentation analysis.

Material	*E* (GPa)	ν	σ_y (MPa)	*n*	Extracted σ_y (MPa)	Extracted *n*
Cu	113	0.30	238¶	0.029	247	0.0193
Al	66	0.33	25¶	0.295	34	0.2487

The experimental tensile load-displacement plots were converted to true stress, σ, and true strain, ε, data and are plotted in Fig. 1. The values of E, σ_y and n measured from the tensile tests are listed in Table 1. Figure 2(a) and (b) show the average indentation curves obtained from the copper and aluminum specimens, respectively. Dao *et al.* [1] and Chollacoop *et al.* [2] have rigorously shown that the loading curvature of the indentation response depends on the reduced Young's modulus and the representative stress only. Thus, the low strain hardening observed in copper implies equal values of representative stress and hence similar indentation curves. Conversely, high strain hardening in aluminum should lead to higher curvature for the loading part of the *P-h* curves with increasing prior plastic strain. The individual *P-h* data were analyzed using the single and dual indenter reverse algorithms detailed in [1,2] and the extracted values of $\sigma_{0.033}$ and $\sigma_{0.057}$ were plotted in Fig. 1, offset by the prior-plastic strain to which the specimens were subjected. It is seen that the uniaxial stress-strain curves are well captured by the predictions from the reverse algorithms.

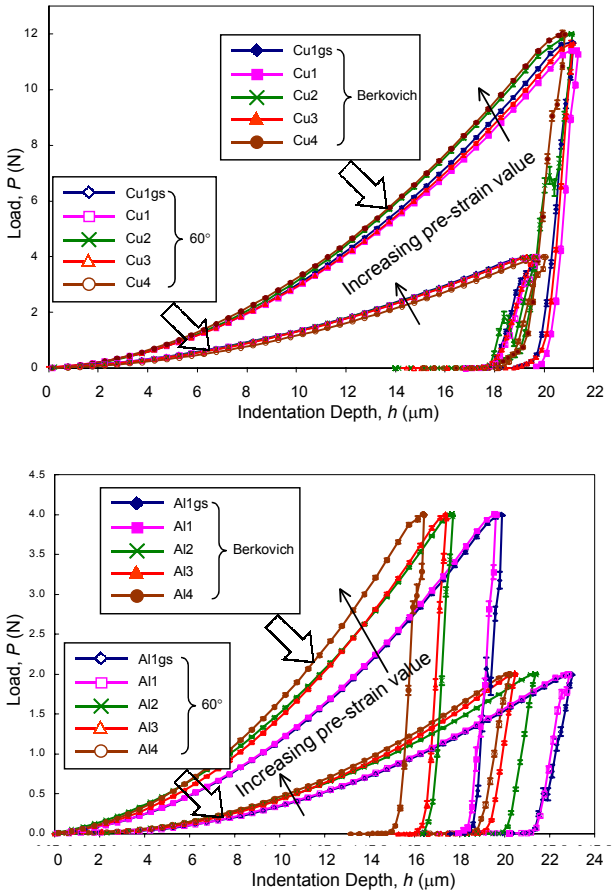

Figure 2: Experimental indentation responses under both Berkovich and 60° cone equivalent three-sided pyramid tips for copper and aluminum specimens.

Tabor [3], on the basis of his experimental observations, proposed that the representative strain introduced within the plastically deformed region, ε_r is ~8% for the case of Vickers indentation. FEM simulations by Giannakopoulos *et al*. [4] suggest that a characteristic strain of 29% separates these two regions of different deformation mechanisms. Chaudhri [5], by conducting a detailed experimental study of subsurface strain distribution around a Vickers indent in Cu, reported that the maximum strain to be in the range of 25–36%, considerably higher than that proposed by Tabor, but in reasonable agreement with the analysis conducted by Giannakopoulos *et al*. Atkins and Tabor [6] have conducted hardness measurements using diamond cones with varying tip angles on copper and mild-steel samples that are work hardened to different levels prior to indentation.. The constrain factor $C(\theta)$ is obtained by dividing the hardness of the specimens subjected to the highest level of pre-strain with the flow stress at that strain. The $H(\theta, n)$ values are then divided by the $C(\theta)$, which is assumed to be independent of the plastic strain and the $\varepsilon_r(\theta)$ is obtained by best fit through the $H(\theta, n)/C(\theta)$ data. The $\varepsilon_r(\theta)$ values thus obtained are plotted in Fig. 3. Subsequent work by Johnson [7] has shown that the constraint factor C is highly sensitive to the E/σ_r as well as E/σ_r ratios, indicating that the basic assumption by Atikins and Tabo [6] that $C(\theta)$ is independent of prior plastic strain (and hence the flow stress in a work-hardening metal) is implicitly incorrect.

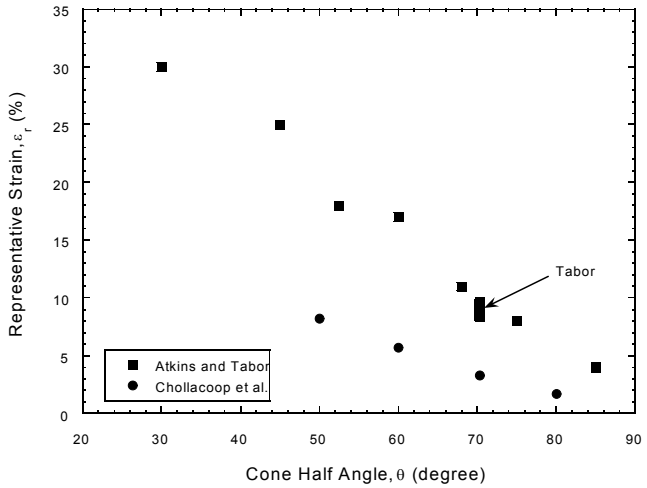

Figure 3: Variation of the representative strain, ε_r, with the indenter tip half angle, θ.

It is instructive to compare the accuracy of the ε_r values estimated by Atkins and Tabor [6]. For this purpose, the hardness values for the indentations made using the 60° cone equivalent three-sided pyramid indenter were estimated by dividing the maximum applied force with the contact area. Then, using the C value given by Atkins and Tabor for this particular geometry (2.42), the flow stress is estimated. They were found to be significantly larger (~100%) than the corresponding extrapolated flow stresses (made assuming power-law) at $(\varepsilon_r + \varepsilon_s)$ with the ε_r for this particular indenter geometry being 17%.

Further, we examined the accuracy of the σ_y and n predictions made using the $\sigma_{0.033}$ and $\sigma_{0.057}$ data. An excellent agreement between the predicted and experimental values of both σ_y and n, for both the copper and the aluminum samples, is noted (Table 1).

4 SUMMARY

Experiments were conducted to critically assess the representative strains underneath sharp indenters, estimated by Dao *et al.* [1] and Chollacoop *et al.* [2] through LFEA for Vickers and conical indenters with varying cone angles, respectively. Two materials of contrasting plastic behavior were plastically strained prior to indentations under both Berkovich and 60° cone equivalent three-sided pyramid tips. A series of $\sigma_{0.033}$ and $\sigma_{0.057}$ were extracted from the single and dual indenter reverse algorithms, which match well with the experimental uniaxial stress-strain data. This representative strain concept allows the possibility to construct the entire stress-strain curves, with better accuracy and less sensitivity, from multiple indentations of one or more indenter tips.

REFERENCES

1. M. Dao, N. Chollacoop, K.J. Van Vliet, T.A. Venkatesh, S. Suresh, Acta Mater. **49,** 3899 (2001).
2. N. Chollacoop, M. Dao, and S. Suresh, Acta Mater. **51,** 3713 (2003).
3. D. Tabor, Hardness of Metals. Oxford: Clarendon Press (1951).
4. A.E. Giannakopoulos, P. L. Larsson, and R. Vestergaard, Int. J. Solids Struct. **31,** 2679 (1994).
5. M.N. Chaudhri, Acta Mater. **46,** 2047 (1998).
6. A.G. Atkins and D. Tabor, J. Mech. Phys. Solids **13,** 149 (1965).
7. K.L. Johnson, J. Mech. Phys. Solids **18,** 115 (1970).